



THERMAL STRESS EVOLUTION OF TUNNEL WALL DURING CONSTRUCTION EVOLUCIJA TERMIČKIH NAPONA U ZIDU TUNELA U IZGRADNJI

Originalni naučni rad / Original scientific paper
Rad primljen / Paper received: 27.09.2023
<https://doi.org/10.69644/ivk-2024-03-0372>

Adresa autora / Author's address:

¹ Institute of Techniques for Special Engineering (ITSE), Le Quy Don Technical University, Hanoi, Vietnam T.C. Nguyen  0000-0001-9723-5161; Q.L. Hoang  0000-0002-9656-0664

*email: trongchuc.nguyen@lqdtu.edu.vn

² Infrastructure Engineering Department, Melbourne University, Australia M. Sofi  0000-0002-0670-9278

Keywords

- temperature field
- thermal stress
- mass concrete
- concrete tunnel
- FEM

Abstract

Thermal stresses resulting from heat of cement hydration during mass structures construction such as dams, transfer slabs, deep beams, and foundation, are the cause of cracks in concrete structures. This paper presents a finite element model representing concrete tunnel lining and evaluates the cracking likelihood due to thermal evolution of early age concrete. The three-dimensional finite element method (3D FEM) is implemented in Midas Civil 2011[®]. The model is used to simulate temperature and thermal stress distribution in the concrete tunnel lining and to conduct a parametric study. The results of the temperature and stress fields are predicted in Vietnam's construction conditions. The above results help engineers before construction to take appropriate measures to control the formation of cracks at an early age.

INTRODUCTION

In recent years, in many developing countries the increase of urban population has resulted to traffic jams. Therefore, it is necessary for urban development to build underground. Tunnel construction is a major undertaking. It involves a combination of earth work and reinforced concrete construction often under confined mechanical and thermal environments. Examples of recent projects include twin tunnels under Yarraville between the West Gate Freeway and the Maribyrnong River, Melbourne Australia /1/, and Kuznetsovskiy tunnel is built in the pass section of Sikhote-Alin Ridge on the Pivan-Sovetskaya Gavan leg of the Far Eastern Railway route, Russia, /2/. Benefits associated with tunnelling are manifold: it moves through traffic away from homes, defers traffic noise underground, decrease of traffic volumes on local streets, eliminates disruption during construction as much of the work happens underground and provides an opportunity for urban development by freeing land on the surface.

Thermal cracking that happens as result of heat generation from hydration of cement is a major factor affecting the quality of construction in the mass concrete reducing its service life. It is now commonly known that the thermal stress resulting from thermal expansion and shrinkage and

Ključne reči

- temperatursko polje
- termički napon
- masivni beton
- betonski tunel
- MKE

Izvod

Termički naponi kao posledica toplote hidratacije cementa tokom izgradnje masivnih konstrukcija kao što su brane, armirano-betonske ploče, zidni nosači, temelji, su uzrok pojave prslina u betonskim konstrukcijama. U radu je predstavljen model konačnim elementima koji opisuje obzid tunela i proračunava mogućnosti za pojavu prslina usled termičke evolucije betona u ranoj fazi. Trodimenzionalna metoda konačnih elemenata (3D MKE) je implementirana u Midas Civil 2011[®]. Model se primenjuje za simulacije raspodele temperature i napona u obzidu betonskog tunela kao i za parametarsku analizu. Data je procena rezultata temperaturskih i naponskih polja u Vijetnamskim uslovima izgradnje. Ovi rezultati pomažu inženjerima pre izgradnje, kako bi preduzeli odgovarajuće mere za praćenje formiranja prslina u ranoj fazi.

the mechanical restraints of the concrete element, induce microcracks in the concrete mass. To reduce the thermal crack resistance in mass concrete, and, hence, to improve durability prospects, fly ash and low-heat cements are normally used to moderate and control temperature rise and thermally induced cracking in-situ concrete, /3, 4/. Addition of fly ash and other supplementary cementitious materials have been found to be effective in reducing alkali silicate expansions, /5, 6/.

Naturally, concrete elements in tunnels are very sensitive to thermal stresses. Newly cast concrete elements are often subject to thermal and mechanical restraints. These conditions make the elements more prone to cracking damage if not carefully managed. Internal damage to structural elements is never welcome. Cracking in the tunnel segments needs be avoided to achieve a low water permeability and ensure that the structure fulfils the demands on service life. To predict the risk of early age thermal cracking in the tunnel during construction, a careful design of the elements is necessary. It is also necessary to monitor the in-situ temperature development and evaluate the level of maturity of the concrete prior to applying structural loads, /7/. In recent years, the most complete factor consideration for the temperature problem solution possibly applies numerical methods,

particularly, finite element methods such as Midas Civil, Ansys, Adina, Abaqus programmes, and others, /8, 9/.

The aim of the paper is to report on the thermal stress modelling and simulation of a typical tunnel shell. The model calculates temperature rise and thermal stress in the tunnel shell during construction. Finite element modelling (FEM) software Midas Civil 2011® is used for this purpose. Only one portion of the tunnel is modelled representing 4 stages of concrete pour to make up the vertical element. The distribution of temperature field and thermal stress field in the tunnel during construction are considered to provide the reasonable references to design and construction of tunnel engineering.

FINITE ELEMENT MODELLING (FEM) APPROACH

Figure 1 shows the cross-section of the immersed tube tunnel built under Vietnamese conditions. The immersed tunnel is an RC structure (width 7.0 m, height 9.0 m, length 7.0 m, bottom and top plate thickness 1.5 m, side wall thickness 1.0 m). As part of design requirements, this structure is meant to have a long durability of 100 years and a waterproof structure not allowed to undergo early age cracking.

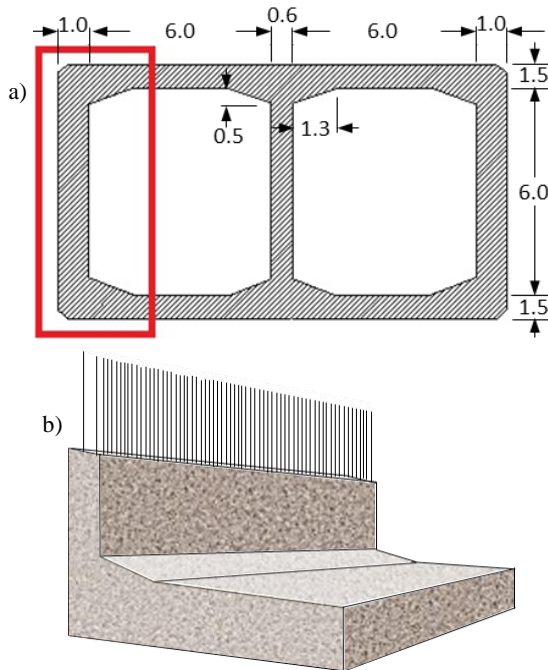


Figure 1. Tunnel dimensions: a) cross-section of the tunnel and dimensions; b) tunnel perspective.

In fact, simulations were carried out before the actual construction in order to predict the workability of concrete, temperature field, thermal stress, and shrinkage strain, and to verify control of thermal cracking.

The governing equation of 3D unsteady heat transfer is based on the principle of energy conservation and Fourier's law of heat conduction and expressed as follows, /10-13/:

$$\frac{\partial}{\partial x} \left(k_x \frac{\partial T}{\partial x} \right) + \frac{\partial}{\partial y} \left(k_y \frac{\partial T}{\partial y} \right) + \frac{\partial}{\partial z} \left(k_z \frac{\partial T}{\partial z} \right) + q_v = \rho c \frac{\partial T}{\partial t} \quad (1)$$

where: T is material temperature (°C); k_x, k_y, k_z are thermal conductivity coefficients of the material dependent on the temperature in directions $x, y,$ and $z,$ in respect (W/m°C); q_v

is the amount of heat released by internal sources (e.g., exothermic heating) to a given moment in time (W/m³); c is specific heat (kJ/kg°C); ρ is concrete density (kg/m³); t is time (day).

Heat transfer boundary conditions: two types of boundary conditions are often used to analyse heat problems, which are given by Eqs. (2) and (3), /14/. Figure 2 shows boundary conditions for the thermal analysis.

$$T = T_p \quad (2)$$

$$k_x \frac{\partial T}{\partial x} l_x + k_y \frac{\partial T}{\partial y} l_y + k_z \frac{\partial T}{\partial z} l_z + q_v + h(T_s - T_f) = 0 \quad (3)$$

where: T_p is the temperature of the surface or foundation °C; q_v is temperature generated per 1 volume unit (kJ/m³); h is convective coefficient (W/m²°C); T_s is the temperature of concrete or foundation (°C); T_f is ambient temperature of the construction area (°C); $l_x, l_y,$ and l_z are directional cosine of the surface according to the $x, y,$ and z axes, respectively.

In this study, part of the tunnel is modelled as a three-dimensional transient heat transfer model using a birth and death procedure to simulate the real construction process of the tunnel. The tunnel is divided into 4 lifts. The sectional view of the placement of concrete lifts is shown Table 1.

The solid element type, available in the Midas Civil 2011 library, is used in finite element analysis. This element is eight nodes solid, with a single degree of freedom, temperature, at each node. Because a mass concrete has symmetry properties, in order to reduce the number of calculations, one-half of it is analysed. The type and dimensions of the investigated concrete block is shown in Fig. 2. The step-by step analysis of the construction simulation process allows the determination of temperature and stress distributions for each added lift.

Table 1. Sectional view of the placement of concrete lifts.

Lift	Part	Height (m)	Curing period (days)
1	bottom slab	+0.00 +1.50	3
2	side wall 1	+1.50 +4.50	3
3	side wall 2	+4.50 +7.50	3
4	top slab	+7.50 +9.00	3

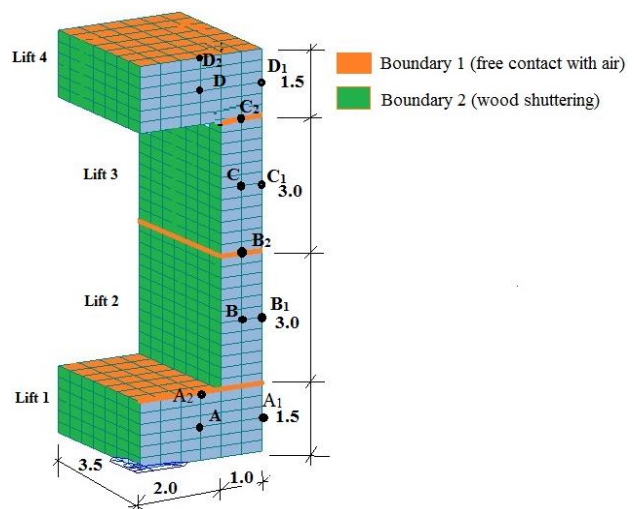


Figure 2. 3-D model for analysis, unit m.

Material properties and environmental conditions

Climate of this region is characterised by fluctuations in air temperature from 21.5 °C in winter to 26.5 °C in summer. The temperature of the foundation under the concrete tunnel is considered 25 °C and initial temperature of concrete mixture when poured is assumed constant at 20 °C. The mix proportion is shown in Table 2. Concrete mixes properties and heavyweight concrete is presented in Table 3. The adiabatic (no heat loss through the boundary) temperature rise according to experiment on concrete at age t is shown in Fig. 3, /15, 16/.

Heat of cement hydration in concrete as a function of time is obtained from several experiments performed in the laboratory. In accordance, the heat of hydration produced with time for Portland cement is shown in Fig. 3, /17/.

Table 2. Mix compositions and properties of fresh concrete, /15/.

Compositions of concrete mixture (kg/m ³)					Properties of fresh concretes		
Cement	Fly ash	Quartz sand	Coarse aggregate	Water	W/C	Average density	Slump (cm)
490	0	545	1108	225	0.46	2368	12

Table 3. Properties of concrete, /15/.

Average compressive strength at different ages (MPa)				Average tensile strength at age of 28 days (MPa)	Elasticity modulus of concrete (N/m ²)	Average density of concrete (kg/m ³)
3 days	7 days	14 days	28 days			
24.3	33.6	41.3	43.1	3.34	3.1×1010	2355

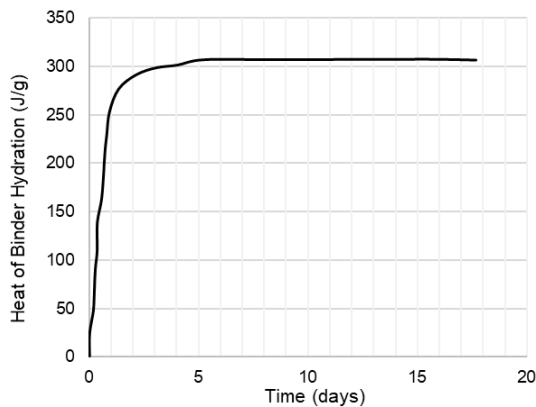


Figure 3. Heat of hydration of Portland cement with time.

The model properties used are considered from available data and typical concrete properties. The density, modulus, Poisson’s ratio, specific heat, and thermal conductivity are given in Table 4.

According to standard ACI 209.2R-08 Guide for modelling and calculating shrinkage and creep in hardened concrete. A creep coefficient and an unrestrained shrinkage strain at any time depend on: age of concrete when drying starts, usually taken as the age at the end of moist curing (days); age of concrete at loading (days); curing method; ambient relative humidity expressed as a decimal; volume-surface ratio or average thickness (m); concrete slump (m); fine aggregate percentage (%); cement content (kg/m³); air content of the concrete expressed in percent (%); an cement type, /18, 19/.

According to the research, /20, 21/, the one-dimensional total strain in concrete can be computed as:

$$\varepsilon_t = \varepsilon_e + \varepsilon_c + \varepsilon_s + \alpha\Delta T, \tag{4}$$

where: ε_e is elastic strain; ε_c is creep strain; ε_s is shrinkage strain; $\alpha\Delta T$ is the thermal dilation.

Table 4. Concrete material properties.

Properties	Value
thermal conductivity coefficient (W/m°C)	2.63
specific heat coefficient (kJ/kg°C)	1.05
mass density (kg/m ³)	2355
boundary 1 (free contact with air) with convection coefficient (W/m ² °C)	10.00
boundary 2 (wood shuttering) with convection coefficient (W/m ² °C)	7.50
elasticity modulus (N/m ²)	3.1×1010
thermal expansion coefficient (1/°C)	0.75×10 ⁻⁵
Poisson’s ratio	0.15
maximum cement hydration heat at 28 days (J/g)	310
unit cement content (kg/m ³)	490
average compressive strength at 28 days (MPa)	43.10
average tensile strength at 28 days (MPa)	3.34

Elastic deformation and creep are dependent on stress σ . Therefore, elastic and creep deformation are written as:

$$\varepsilon_e + \varepsilon_c = \frac{\sigma(t)}{E(t)} + \sigma(t)C(t, t_0) = \sigma(t)J(t, t_0), \tag{5}$$

where: $J(t, t_0)$ is creep compliance (MPa⁻¹),

$$J(t, t_0) = \frac{1}{E(t)} + C(t, t_0). \tag{6}$$

The modulus of elasticity $E(t)$ of concrete is dependent on the age t . Currently, there are many models to predict shrinkage and creep in concrete, as ACI 209R-92 model, Bažant-Baweja B3, CEB MC90, CEB MC90-99, and GL 2000. The prediction of tensile creep at early age due to restrained drying and autogenous shrinkage requires careful re-examination of these equations. In this study, the ACI 209R-92 model is used to predict shrinkage and creep in concrete.

Shrinkage strain $\varepsilon_s(t, t_0)$ is modified by correction factors for relative humidity, duration of drying, slump, cement content, aggregate, and air content. In ACI 209R-92 model code, the shrinkage strain of concrete can be calculated by:

$$\varepsilon_{sh}(t, t_0) = \frac{(t-t_0)^\alpha}{f_c + (t-t_0)^\alpha} \varepsilon_u^s, \tag{7}$$

where: t_0 is time at which drying begins; f_c , α are constants; ε_u^s is the ultimate shrinkage.

The creep model proposed by ACI 209R-92, gives creep strain of concrete by the following formula,

$$\phi(t, t_0) = \frac{(t-t_0)^\psi}{d + (t-t_0)^\psi} \phi_u, \tag{8}$$

where: $\phi(t, t_0)$ is the creep coefficient at concrete age t due to a load applied at the age t_0 ; d , ψ are constants for a given member shape and size that define the time-ratio part; $(t - t_0)$ is the time since application of load; ϕ_u is the ultimate creep coefficient. The Midas Civil® software helps to declare parameters needed to mention creep of concrete at early age days.

RESULTS AND DISCUSSION

Midas civil software based on finite element principles is used to determine the temperature and thermal stress in mass concrete with different construction conditions. Midas solves many different structural problems including the temperature transmission problem in a structure. The results of the analysis are shown in Figs. 4-8.

The determination of temperature fields in early age mass concrete is a complex problem because it not only depends on the shape of the structure, but it also depends on factors such as internal (cement hydrothermal heat) and outside (construction conditions, ambient temperature changes).

- First lift

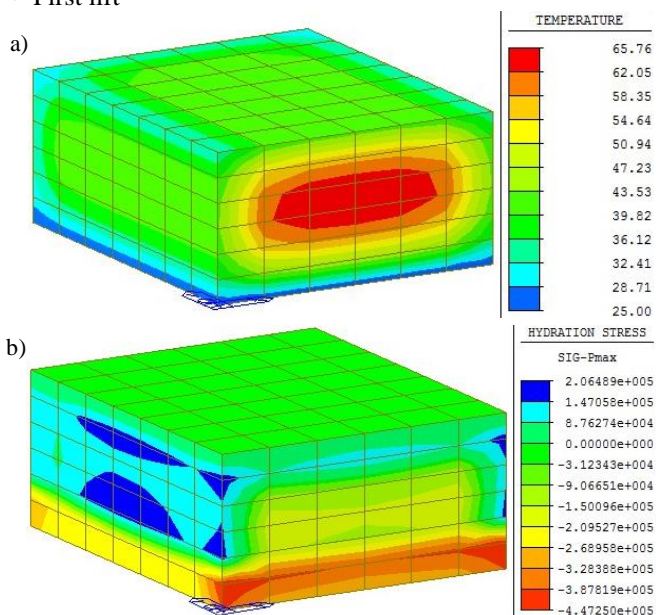


Figure 4. Temperature field (a) and thermal stress state (b) at the centre of concrete bottom slab of the tunnel, 48 hours after construction (first lift).

From the results shown in Fig. 4a, it follows that the maximal temperature at the centre of the concrete bottom slab of the tunnel at 48 hours after its construction, $T_{max} = 65.76 \text{ }^\circ\text{C}$. After that, the temperature begins to decrease. The temperature development at points: the central (A), surface of side edge (A_1), and surface of the top (A_2) of the first lift are shown in Fig. 5. This is the portion of the tunnel that is freely sitting without any thermo-mechanical restrains. All surfaces are covered by plywood and surfaces are exposed to ambient conditions.

Also, from Fig. 4b, it is seen that the maximum tensile stress on the outer side surface and the bottom slab of the tunnel is 2.06 MPa, which does not exceed the tensile strength of concrete, equals 3.34 MPa (Table 3). Hence, there are no cracks forming under these conditions.

The temperature difference between the centre and the surface causes the tensile stress to form. Figure 5 shows that the maximal temperature difference between centre (A) and surface (A_1 , A_2) of the concrete block is $21.05 \text{ }^\circ\text{C}$. The temperature differences may be within the permitted range (CIRIA C660). In order to conclude, the formation of cracks is necessary to determine the thermal stress at the time of the maximal temperature difference.

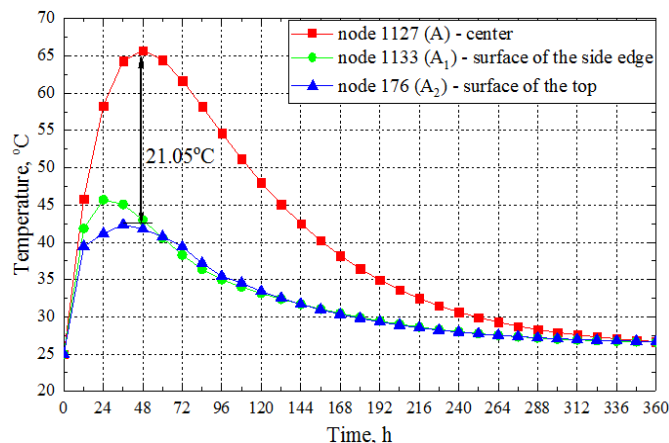


Figure 5. Temperature development at points A, A_1 , and A_2 of the concrete bottom slab (first lift).

- Second lift

The second stage of the simulation reports on the construction of the first half of the wall. From bottom, this wall is supported by the slab that is constructed in the previous step. The half wall is supported by formworks on four sides. It is exposed to air at the top surfaces. From the results shown in Fig. 6a, it follows that the maximum temperature at the centre of the concrete side wall (+1.5 to +4.5) of the

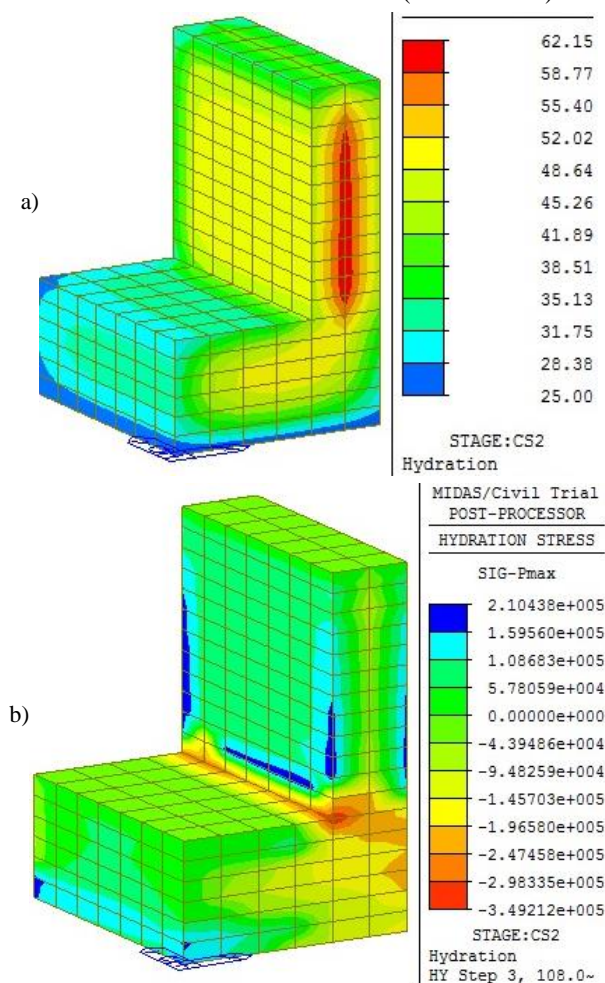


Figure 6. Temperature field (a) and thermal stress state (b) at the centre of concrete side wall (+1.5 to +4.5) of the tunnel, 108 hours after construction (second lift).

tunnel after 108 hours of concrete hardening is $T_{max} = 61.15$ °C. After that, the temperature also begins to decrease.

From Fig. 6b it is clearly seen that the maximum tensile stress on the outer side surface of the concrete side wall (+1.5 to +4.5) of tunnel, equals 2.1 MPa which does not exceed the tensile strength of concrete. So, on the outer surface side wall of the tunnel cracks do not form.

Figure 7 shows the temperature development over time at points B, B₁, and B₂ of concrete side wall (+1.5 to +4.5) of the tunnel (second lift). The difference between the centre and the surface of concrete blocks is 22.03 °C. The value of temperature difference exceeds permissible values (20 °C). Therefore, the risk of cracking is higher in the surface (B₂) of the concrete side wall.

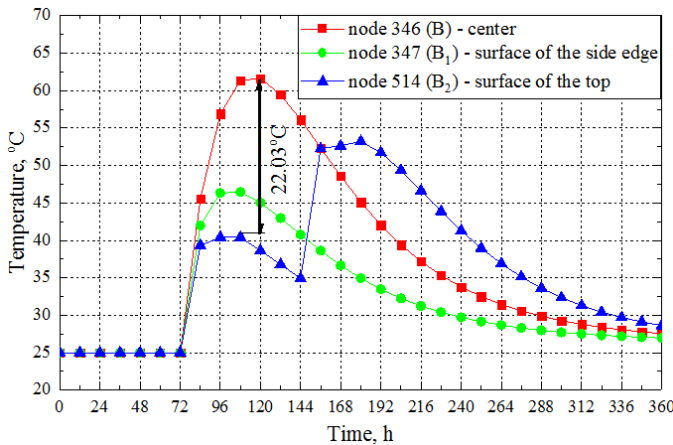


Figure 7. Temperature development at points B, B₁ and B₂ of the concrete side wall (+1.5 to +4.5) of the tunnel (second lift).

• Third lift

Like the second lift, the third stage of simulation shows the construction of the second half of the wall element. From results shown in Fig. 8, it follows that the maximum temperature at the centre of the concrete side wall (+4.5 to +6.0) of the tunnel after 192 hours of concrete hardening is $T_{max} = 61.67$ °C (Fig. 8a).

Also, from Fig. 8b it is clearly seen that the maximum tensile stress on the outer side surface of the concrete side wall of the tunnel, equals 7.45 MPa, also exceeds the tensile strength of concrete in bending. The stresses at the bottom of the bottom slab reach a relatively large value because there, a displacement constraint is required. Thus, in these

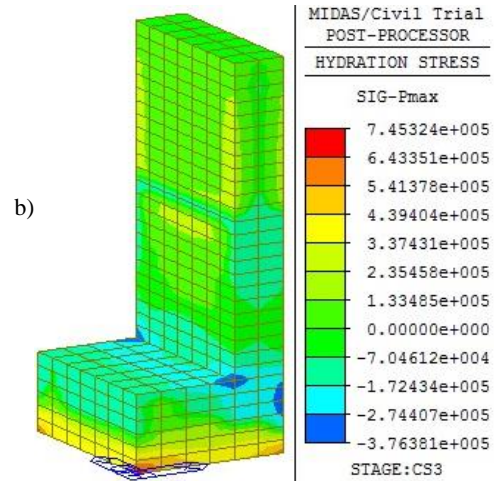
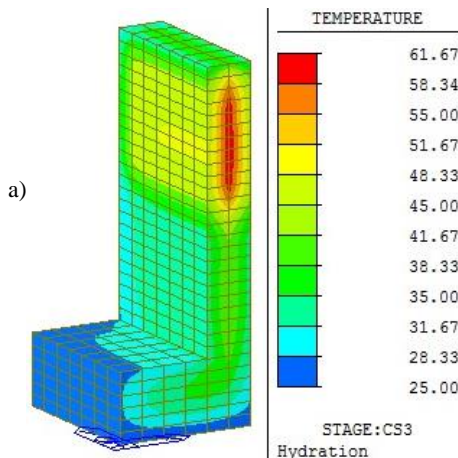


Figure 8. Temperature field (a) and thermal stress state (b) at the centre of concrete side wall (+4.5 to +6.0) of tunnel, 192 hours after construction (third lift).

places on the outer surface side wall of the tunnel there are also conditions for the appearance of cracks due to the release of heat during the hydration of cement.

Figure 9 shows that the temperature difference between the centre and surface of concrete block is 25.04 °C. This shows the risk of forming surface cracks in the 3rd stage of the tunnel wall construction process.

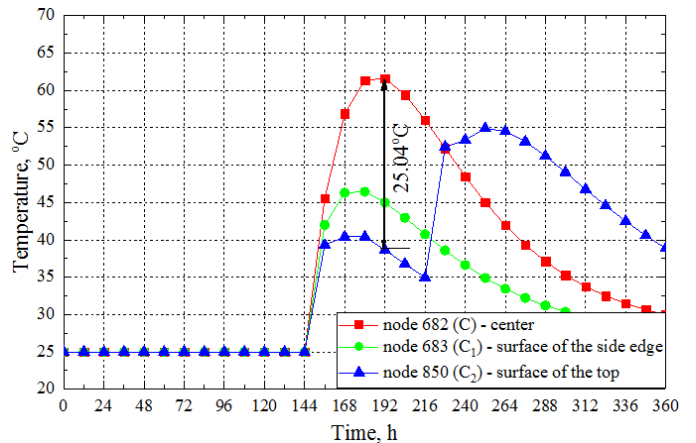


Figure 9. Temperature development at points C, C₁, and C₂ of concrete side wall (+4.5 to +6.0) (third lift).

• Fourth lift

From the results shown in Fig. 10, it follows that the maximal temperature at the centre of the concrete top slab (+6.0 to +9.0) of the tunnel after 264 hours of concrete hardening is $T_{max} = 69.51$ °C, Fig. 10a, due to the top surface of the concrete top slab directly in contact with air. Therefore, their temperature drops faster than the temperature in the centre. This leads to a large temperature difference (28.5 °C) and is shown in Fig. 11. Because the temperature difference exceeds the allowed value, the risk of cracking on the surface is very high. For a detailed evaluation, it is necessary to determine the thermal stress field.

Also, from Fig. 10b it is clear that the maximum tensile stress on the outer side surface of the tunnel, equal to 10.43 MPa, also exceeds the tensile strength of concrete in bending. Thus, at these places on the outer surface side of the tunnel there are also conditions for the appearance of cracks.

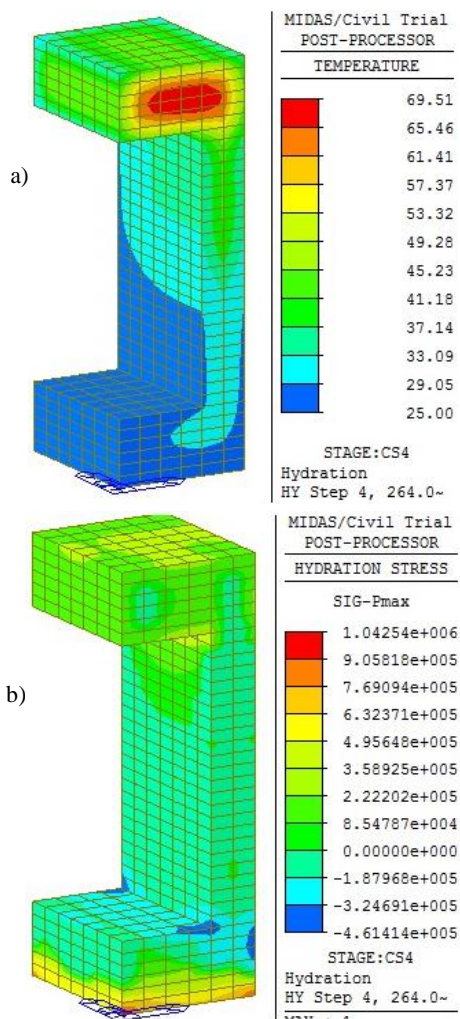


Figure 10. Temperature field (a) and thermal stress state (b) at the centre of concrete top slab (+6.0 to +9.0) of tunnel, 264 hours after construction (fourth lift).

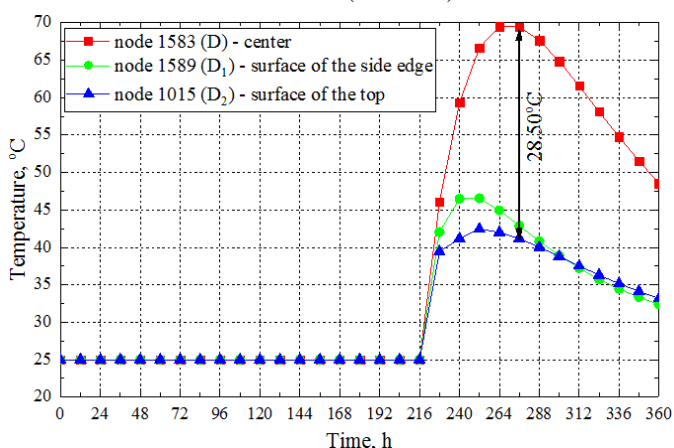


Figure 11. Temperature development at points D, D₁, and D₂ of concrete top slab (+6.0 to +9.0) (fourth lift).

Figure 12 shows the principal temperature at the centre of the blocks for the real construction process of the tunnel. The maximal temperature recorded after the end of construction was 69.51 °C in the top slab of the tunnel.

Table 5 shows that at the third- and fourth lift of tunnel construction, at 192 hours and 264 hours, cracks formed on the face tunnel.

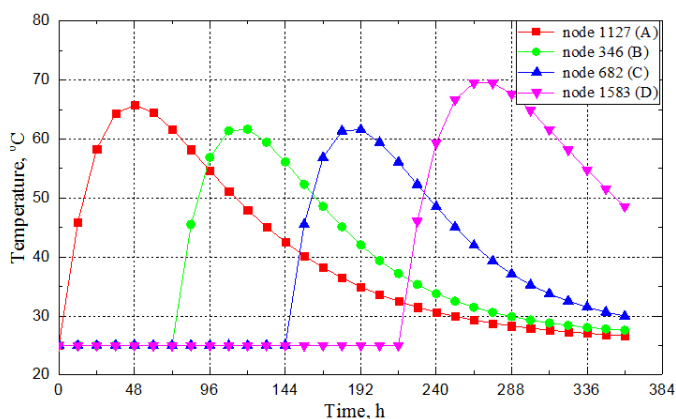


Figure 12. Temperature development at points (A-node 1127, B-node 346, C-node 682, D-node 1583) of the tunnel.

Table 5. Maximum temperature, thermal stress, and time of appearance during construction.

Part	Lift 1	Lift 2	Lift 3	Lift 4
Maximal temperature at the centre (°C)	65.76	62.15	61.67	69.51
Maximal tensile stress (MPa)	2.06	2.10	7.45	10.43
Maximal temperature occurrence time (hours)	48	108	192	264
Appearance of cracking in structure	no cracking	no cracking	cracking	cracking

For daily monitoring of tunnel concrete construction, the evaluation of different levels of loading is very important as it indicates that compressive and tensile stresses are happening at different stages of the construction. Due to changing weather conditions and thermomechanical restraints, the stresses resulting from thermal and other early-age related strains can cause fine cracks and consequently reduce the permeability of concrete materials. From the analysis reported in this paper it can be seen that the stresses are relatively low, and they are not likely to cause failure of tunnel concrete materials. This paper presents stress-based loading after panel concrete segments and discusses the likelihood of cracks happening based on the temperature differentials. However, since moisture can be readily available to infiltrate minor cracks, should they happen, they will result in reducing the durability of the tunnel. Hence, the type of calculation presented in this case study becomes important.

CONCLUSION

Based on the results of the study, the following conclusions can be obtained.

- The software complex Midas Civil 2011® is a fairly effective tool for calculating the temperature regime and the thermally stressed state of concrete structures during their construction.
- Using the Midas Civil 2011® computer programme, the maximal temperatures in the central zone of the concrete tunnel are determined in all four steps of the tunnel construction, which were 65.74 °C after 48 hours, 62.15 °C after 108 hours, 61.67 °C after 192 hours, and 69.51 °C after 264 hours from the start of mixing the mixture of raw materials with water.
- At the third and fourth lift of the tunnel construction at 192 and at 264 hours of hardening of concrete, the tensile

stress on the outer side and at the bottom of the structure exceeds the tensile strength of concrete in bending, which can lead to the formation of cracks.

Therefore, to prevent cracking in the tunnel being built, it is necessary to care for the concrete during its hardening, especially at an early age.

REFERENCES

- Mcneil, J., Pillot, D., Voelske, A., Burke, R. (2021), *Westgate tunnel, Melbourne family of footbridges for a tunnel project*, In: J. Romo (Ed.), Conf. Proc.: Footbridge Madrid 2022 - Creating Experience, Madrid, Spain, Asociación Española de Ingeniería Estructural (ACHE), 2022. doi: 10.24904/footbridge2022.042
- Kvashuk, S., Smyshlyayev, B., Trunev, V. (2019), *Peculiarities of mining and technical conditions for construction and operation of Kuznetskovskiy tunnel on the far eastern railway*, MATEC Web Conf. 265: 05016: doi: 10.1051/mateconf/201926505016
- Sofi, M., Lumantarna, E., Mendis, P., Zhong, A. (2019), *Thermal stresses of concrete at early ages*, J Mater. Civ. Eng. 31 (6): 04019056. doi: 10.1061/(ASCE)MT.1943-5533.0002684
- Sofi, M., Mendis, P.A., Baweja, D. (2012), *Estimating early-age in situ strength development of concrete slabs*, Constr. Build. Mater. 29: 659-666. doi: 10.1016/j.conbuildmat.2011.10.019
- Rupasinghe, M., Mendis, P., Ngo, T., et al. (2017), *Compressive strength prediction of nano-silica incorporated cement systems based on a multiscale approach*, Mater. Des. 115: 379-392. doi: 10.1016/j.matdes.2016.11.058
- Sturup, V.R., Hooton, R.D., Clendenning, T.G. (1983), *Durability of fly ash concrete*, In: Fly Ash, Silica Fume, Slag and Other Mineral By-Products in Concrete, Vol. 1, V.M. Malhotra (Ed.), ACI SP-79, American Concrete Institute, Detroit, pp.71-86.
- Sofi, M., Mendis, P., Baweja, D., Mak, S. (2014), *Influence of ambient temperature on early age concrete behaviour of anchorage zones*, Constr. Build. Mater. 53: 1-12. doi: 10.1016/j.conbuildmat.2013.11.051
- MIDAS Information Technology, (2011), Heat of Hydration - Analysis Manual: 256 p.
- Liu, X., Yuan, Y., Su, Q. (2014), *Sensitivity analysis of the early-age cracking risk in an immersed tunnel*, Struct. Concrete, 15(2): 179-190. doi: 10.1002%2Fsuco.201300064
- Japan Concrete Institute (2017), Guidelines for control of cracking of mass concrete, 2016. Japan, 302 p.
- Nguyen, T.C., Huynh, T.P., Tang, V.L. (2019), *Prevention of crack formation in massive concrete at an early age by cooling pipe system*, Asian J Civ. Eng. 20(8): 1101-1107. doi: 10.1007/s42107-019-00175-5
- Lee, M.H., Chae, Y.S., Khil, B.S., Yun, H.D. (2014), *Influence of casting temperature on the heat of hydration in mass concrete foundation with ternary cements*, Appl. Mech. Mater. 525: 478-481. doi: 10.4028/www.scientific.net/AMM.525.478
- Khanzaei, P., Abdulrazeg, A.A., Samali, B., Ghaedi, K. (2015), *Thermal and structural response of RCC dams during their service life*, J Therm. Stress. 38(6): 591-609. doi: 10.1080/01495739.2015.1015862
- Yikici, T.A., Chen, R.H.L. (2018), *2D modeling temperature development of mass concrete structures at early age*, In: Hordijk, D., Luković, M. (Eds.), High Tech Concrete: Where Technology and Engineering Meet, Springer Cham: 612-620. doi: 10.1007/978-3-319-59471-2_73
- Lam, T.V., Nguyen, T.C., Hung, N.X., et al. (2018), *Effect of natural pozzolan on strength and temperature distribution of heavyweight concrete at early ages*, MATEC Web of Conf. 193: 03024. doi: 10.1051/mateconf/201819303024
- Nguyen, T.C., Lam, T.V., Bulgakov, B.I. (2018), *Designing the composition of concrete with mineral additives and assessment of the possibility of cracking in cement-concrete pavement*, Mater. Sci. Forum, 931: 667-673. doi: 10.4028/www.scientific.net/MSF.931.667
- Malkawi, A.I.H., Mutasher, S.A., Qiu, T.J. (2003), *Thermal-structural modeling and temperature control of roller compacted concrete gravity dam*, J Perform. Constr. Facil. 17(4): 177-187. doi: 10.1061/(ASCE)0887-3828(2003)17:4(177)
- ACI 209.2R-08, (2008), Guide for Modeling and Calculating Shrinkage and Creep in Hardened Concrete. American Concrete Institute. ISBN 978-0-87031-278-6
- Nguyen, T.C., Luu, X.B. (2019), *Reducing temperature difference in mass concrete by surface insulation*, Mag. Civ. Eng. 88 (4): 70-79. doi: 10.18720/MCE.88.7
- Wei, Y., Liang, S., Guo, W. (2017), *Decoupling of autogenous shrinkage and tensile creep strain in high strength concrete at early ages*, Exper. Mech. 57(3): 475-485. doi: 10.1007/s11340-016-0249-8
- Bamforth, P.B., Early-Age Thermal Crack Control in Concrete, CIRIA C660, London, 2007. ISBN 978-8-86107-660-2

© 2024 The Author. Structural Integrity and Life, Published by DIVK (The Society for Structural Integrity and Life 'Prof. Dr Stojan Sedmak') (<http://divk.inovacionicentar.rs/ivk/home.html>). This is an open access article distributed under the terms and conditions of the Creative Commons Attribution-NonCommercial-NoDerivatives 4.0 International License